ICESat-2 Lidar Estimates of Clear-Sky Precipitation over the East Antarctic Plateau

Stephen P. Palm
Science Systems and Applications, Inc., Lanham, MD 20706
Stephen.p.palm@nasa.gov

Yuekui Yang
NASA Goddard Space Flight Center, Greenbelt, MD 20771
Yuekui.yang-1@nasa.gov

Abstract

Precipitation over Antarctica plays a critical role in determining the mass balance of the ice sheet, yet it remains poorly quantified due to the harsh environment and sparse number of observations. Over the East Antarctic Plateau, clear-sky precipitation (CSP) is a significant portion of the total annual precipitation. CSP consists of very small ice crystals that form when the air becomes supersaturated and settle to the surface. This study presents the first continental-scale estimates of CSP over the East Antarctic Plateau using atmospheric backscatter profiles from the ICESat-2 lidar. A method is developed to identify CSP based on calibrated attenuated backscatter and to estimate the associated precipitation amounts by deriving ice water content from lidar extinction and using an estimated particle fall speed to obtain precipitation rate. Comparisons with in-situ measurements at Concordia Station, Dome C show general agreement. Results for the April–October 2021 period reveal a high frequency of CSP (up to 80%) across the high Plateau. The ICESat-2 estimated CSP amount for this period ranges from about 5-8 mm SWE south of about 80S and increases toward the north with maximum values of 18-20 mm SWE near 70S, 90E. The ICEsat-2 estimated CSP amount for the grid box containing Dome C was 8.5 mm SWE which agrees well with the amount measured there (9.9 mm SWE). These findings demonstrate the unique ability of ICESat-2 to detect and quantify CSP, offering new insight into Antarctic precipitation and providing a valuable dataset for evaluating the surface mass balance of Antarctica.

Key Points

A method is developed that utilizes ICESat-2 calibrated, attenuated backscatter to derive the spatial frequency and amount of clear-sky precipitation over the Antarctic Plateau.

We find the frequency of clear-sky precipitation is greater than 70% over the Antarctic plateau and is related to elevation

The amount of clear-sky precipitation during the study period is between 8 – 16 mm SWE with a distinct south to north gradient

Plain Language Summary

Antarctica is roughly one and a half times as large as the United States and contains nearly ¾ of the earth's fresh water in the form of the Antarctic ice sheet. As the climate warms, melting of the ice sheet could contribute to sea level rise if it exceeds the amount of snowfall. Due to a lack of observations the amount of precipitation falling over the Antarctic continent is not well known. Satellite radar such as CloudSat has provided the most comprehensive measurements of Antarctic precipitation but is unable to resolve a very light but widespread form of snowfall called clear-sky precipitation or CSP. CSP is composed of very small ice crystals that form in otherwise clear air and is very common over a large portion of Antarctica. The work presented here develops a method to detect the presence of CSP and estimate its spatial distribution, frequency and amount using lidar backscatter profiles from the ICESat-2 satellite. We find that CSP accounts for a large fraction of the precipitation falling over much of the Antarctic Plateau. This work increases our understanding of Antarctic precipitation and represents the first time CSP has been detected and quantified using satellite lidar.

1 Introduction

The vast continent of Antarctica contains nearly ¾ of earth's fresh water. Knowledge of the mass balance of the Antarctic ice sheet is crucial to determining how a changing climate will affect that balance and as a result sea level rise. Precipitation over Antarctica is the single most important factor controlling the mass balance of the ice sheet and yet, due to the lack of observations and environmental difficulties (i.e. high winds, blowing snow), is poorly known. This is especially true over the high East Antarctic Plateau where there are virtually no observations. Most Antarctic precipitation occurs within a few hundred km of the coast and is a result of cyclonic and frontal activity (Bromwich, 1988). The majority of these storm

systems do not penetrate far enough inland to reach the higher portions of the continental interior. These areas are essentially a desert and current knowledge suggests that large regions receive less than 100 mm snow water equivalent (SWE) of precipitation per year and some areas less than 50 mm (Palerme et al., 2017). In these regions a large portion of the precipitation is thought to be the result of clear-sky precipitation (CSP). Clear-sky precipitation can be defined as the fall of non-branched ice crystals in the form of thin hexagonal plates, columns, needles and triangular crystals in otherwise clear skies (Santachiara et al., 2015). CSP forms when the air becomes supersaturated with respect to ice at very cold temperatures and often happens through radiative cooling of the air during the long Antarctic winter. Sometimes these ice crystals are referred to as diamond dust (DD) and some authors may use the terms interchangeably. It is thought that DD and CSP form mainly in the inversion layer where temperatures are generally the coldest (Walden et al., 2003), but over Antarctica there are few if any observations of its vertical extent.

In the Arctic the characteristics of DD were studied using data from the SHEBA field campaign (Intrieri and Shupp, 2004). They found that DD occurred 13% of the time between November 1997 and 10 May 1998 at the SHEBA ship located in the south-central Arctic Ocean. Further, DD was not observed at all between 11 May and 2 October 1998. Using ship-based lidar, they found that DD vertical extent rarely exceeded 1 km with a mean depth of 250m. However, lidar measurements at the South Pole indicate that diamond dust associated with clear-sky precipitation can extend a few km in the vertical (Smiley et. al., 1980).

The conditions necessary for CSP formation occur frequently in winter over much of East Antarctica. In fact, at Plateau Station, near the crest of the East Antarctic ice sheet, Radok and Lile (1977) estimated that 87% of the 1967 precipitation over the station came from CSP. Ground based lidar observations of CSP at the south pole frequently showed elevated backscatter layers exceeding 1000 m in depth and often the presence of a formation layer overlying the precipitation layer, indicating seeding of precipitating ice crystals from above (Smiley et al., 1980). In other areas of the Plateau such as Dome Fuji the total precipitation amounted to only 27.5 mm (SWE) over the period 3 February 2003 to 20 January 2004

(Dittmann et al., 2016). Most of this was the result of CSP and the highest observed daily precipitation was 2.1 mm (SWE). Further, the mean daily precipitation was 0.08 mm w.e. and only 24 days had no precipitation observed, suggesting CSP as being the most frequent form of precipitation. Hogan (1976) noted that the annual precipitation at South Pole Station was 7 cm (SWE) and ice crystal precipitation (or CSP) was very frequent. He noted that usually CSP amounted to a trace, but occasionally an amount of 3 mm (SWE) accumulated in a matter of hours in calm conditions. Walden et al. (2003) reported a 91% frequency of occurrence of these slowly precipitating crystals during 6 winters at the South Pole. At Vostok station CSP was almost a daily occurrence where diamond dust has been estimated to contribute 75 ± 16% of the annual mass accumulation (Ekaykin et al., 2004). It should also be noted diamond dust formation is not necessarily restricted to clear sky conditions and may also occur below high cloud cover (Stenni et al., 2016).

While the above observations indicate that over some areas of the high Antarctic Plateau the majority of precipitation falls as CSP, there currently is no way to reliably detect it or estimate how much has fallen over a large area. Satellite radar remote sensing has likely given the most complete picture of Antarctic precipitation but has difficulty detecting very light precipitation and CSP. For instance, the CloudSat radar operating at 94 GHz cannot detect much of the CSP because the particles are too small and diffuse. Grenier et al., (2009) compared simultaneous backscatter measurements of Antarctic clouds by the CALIOP lidar and CloudSat radar. Their work indicated that CloudSat cannot detect clouds below an average 532 nm backscatter coefficient of about 1.0×10^{-5} $m^{-1}sr^{-1}$. As the data presented in this paper will show, the 532 nm backscatter coefficient of CSP is mostly below this level, indicating CloudSat could not detect it. CloudSat also has trouble retrieving shallow precipitation below 1 km above the surface due to ground clutter. Satellite lidar, operating in the visible portion of the spectrum, is sensitive enough to detect the small and diffuse ice crystals comprising CSP and has no or minimal ground clutter problem. Detecting the presence of CSP with lidar is certainly possible, but can it also estimate an amount of precipitation directly from lidar backscatter measurements? This study intends to answer this question using the Ice, Cloud and land Elevation Satellite-2 (ICESat-2) atmospheric

backscatter profiles and near-coincident ground-based measurements of CSP at Dome C on the East Antarctic Plateau.

For this study, clear-sky precipitation is defined as enhanced lidar backscatter in contact with the surface. Enhanced backscatter is defined as the average backscatter in the lowest 1 km above the surface that exceeds 2 times the molecular scattering value (i.e. 2 times $1.0x10^{-6}$ $m^{-1}sr^{-1}$ over the Antarctic Plateau). For most of these cases the average 1 km backscatter is less than $1.0x10^{-5}$ $m^{-1}sr^{-1}$. The vertical extent of the enhanced backscatter usually exceeds 1 km and can be many kms in depth, but the average optical depth of the entire layer is usually less than 0.3. The instances of vertically extensive (kms thick) enhanced backscatter could more aptly be defined as cirrus or cirrus-like clouds in contact with the ground. Given that it is difficult to distinguish between CSP and thin cirrus in contact with the surface from satellite lidar, we include such cases as clear-sky precipitation. This definition would then include the conventional cases of CSP and those more associated with thin clouds. The fact that multiple observers use the phrase "in otherwise clear skies" in their descriptions of CSP indicates that clouds, if present, are very optically thin, like those included in our analysis.

Section 2 of this paper describes the data and analysis methods used to estimate CSP from ICESat-2 lidar data and a comparison of ICESat-2 retrieved CSP amount with Dome C measurements. Section 3 presents the spatial distribution of the frequency and amount of CSP over the East Antarctic Plateau and section 4 gives a brief discussion of precipitation retrieval uncertainty. Discussion and conclusions follow in sections 5 and 6.

2. Data and Methods

2.1 ICESat-2

ICESat-2, the successor to ICESat, was launched into a 92° inclination orbit in September of 2018 and has been in continuous operation since October of that year (Abdalati et al., 2010; Markus et al., 2017). Though specifically designed and optimized to obtain high resolution altimetry measurements of the Earth's surface, ICESat-2 also has an atmospheric channel to record backscatter from molecules, clouds and aerosols. ICESat-2 carries only one

instrument – the Advanced Topographic Laser Altimeter System (ATLAS) that utilizes a high repetition rate (10 KHz), low per pulse energy (500 μJ), 532 nm laser and photon counting detectors. The laser pulse is split into 6 simultaneously emitted beams by a diffractive optical element (DOE). For more information on the ICESat-2 atmospheric data and first results, please see Palm et al., (2021). This study utilizes the version 006 ATL09 data product containing calibrated, attenuated backscatter (CAB) profiles that consist of 30 m bins extending nominally from 13.5 km above local ground level to 0.5 km below the surface (Palm et al., 2021). The ATL09 product contains 3 such profiles separated by about 3 km and profile number 1 is used here.

2.2 Concordia Station at Dome C

Dome C is the site of Concordia Station (75.1S, 123.3E; elevation 3233 m a.s.l.), which is a French-Italian research facility located on the East Antarctic Plateau open all year round since 2005. Observations of atmospheric variables including precipitation are recorded daily (Grigioni et al., 2022). The precipitation sampling site is located in an area, approx. 800 m from Concordia Station. Precipitation accumulates over an 80x120 cm wooden platform standing 1 m above the snow surface. The platform is covered by a polystyrene/polytetrafluoroethylene surface and is shielded by an 8-cm rail to prevent snow from being blown off from the surface. Samples are manually collected at approximately 10 AM local time (2 UTC) each day by removing all the accumulated material, melting it and determining its mass (Dreossi et al., 2024, 2025). The Dome C precipitation data would include instances of hoar frost. In such cases the reported precipitation is extremely small and for the work done in this paper, we eliminate cases where the reported precipitation is less than 0.01 mm. The site also has an upward pointing ceilometer that gives continuous measurements of backscatter as a function of height and radiosondes are launched daily (weather permitting) at 12 UTC. An automated weather station (AWS) at Dome C records surface temperature, wind velocity and relative humidity on an hourly basis.

2.3 ICESat-2 Precipitation Estimation Method

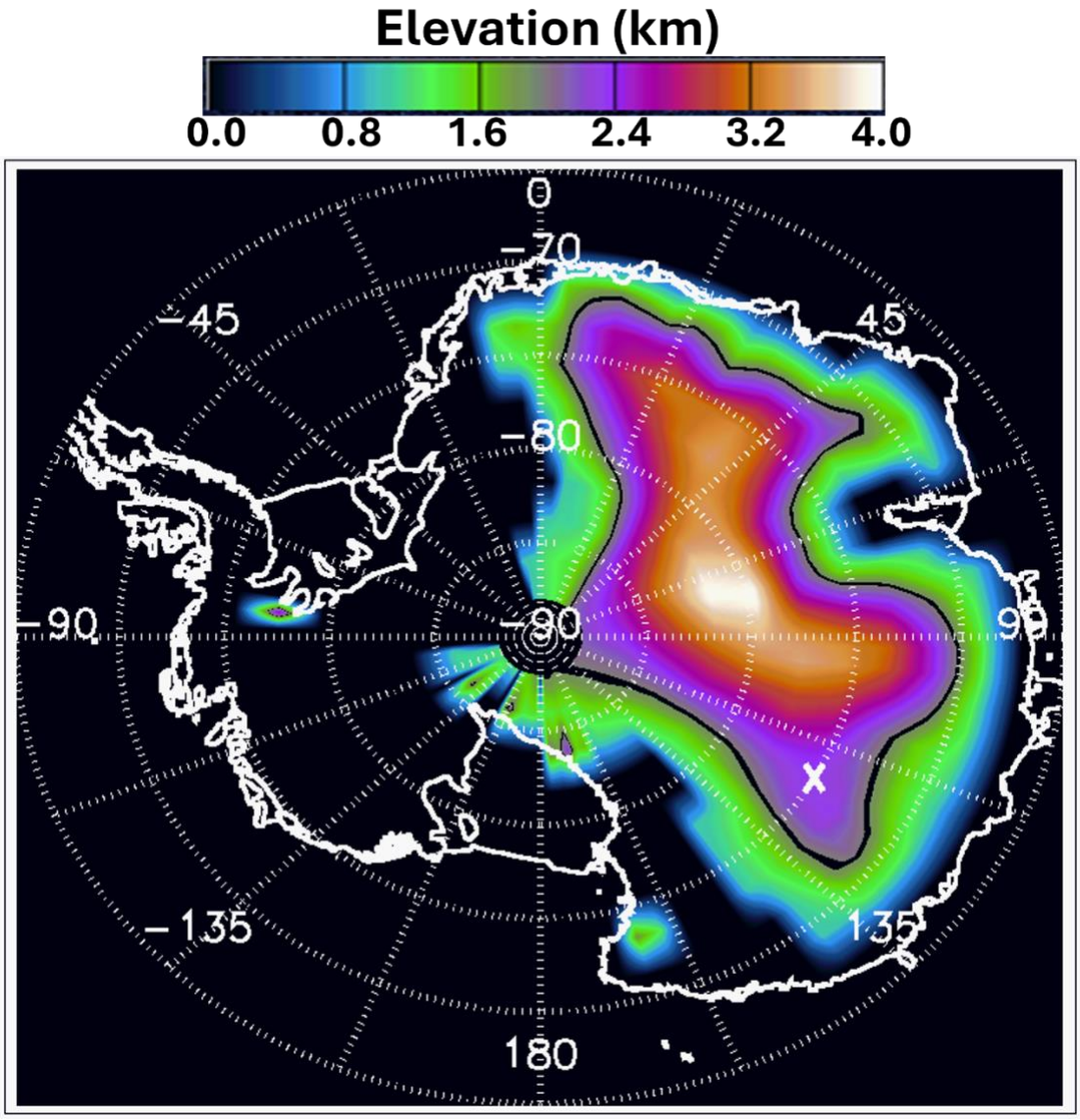

Figure 1. *Color coded elevation around the study area. The black line within the colored area represents the 2500 m elevation contour and the white 'X' the location of Dome C..*

A grid with horizontal resolution of 2 degrees latitude by 4 degrees longitude (roughly 220 km by 120km at 75S) is established over Antarctica. The grid covers 360 degrees of longitude and extends from 70S to 88S but only grid boxes at or above 2500 m in elevation are used for the analysis (see Figure 1). For each ICESat-2 pass over Antarctica within the period being considered, all CAB profiles that contain a valid surface return that fall within a given grid box are used to compute the average CAB between the surface (or top of the blowing snow layer if present) and 1 km above the surface. It is important to exclude the scattering from blowing

snow layers in the 1 km average since the blowing snow can be confused with CSP and generally has a much higher CAB magnitude than CSP. The ICESat-2 ATL09 data product contains detected blowing snow layers and is used for this purpose.

If the 1 km average CAB is greater than a threshold (2 times the 1 km avg molecular backscatter value), then the 1 km average CAB value is added to the sum of all such CAB values in the grid box. The threshold was determined by a trial-and-error process. The threshold must be low enough to capture very diffuse ice particles yet above a level where noise could cause the selection of actual clear profiles. A number of runs were made starting with a high threshold and the selected profiles were then examined in image form (like Figure 2). The threshold was then incrementally reduced until clear profiles began being included. The point at which clear profiles were entirely eliminated determined the threshold. A count of the number of 1 km average CAB values greater than the threshold is kept and if it exceeds 50 (50 ICESat-2 backscatter profiles correspond to a 14 km horizontal distance), then CSP is assumed present in the grid box. In this case, the average of the 1 km average CAB values is used to compute the extinction using an extinction to backscatter ratio (S) of 30 sr. If the count of the 1 km average CAB values greater than the threshold is less than 50, no CSP is assumed, and the extinction is set to zero for that pass over the grid box. An example of the set of CAB profiles used to compute the extinction from the lowest 1 km average CAB is shown in Figure 2a.

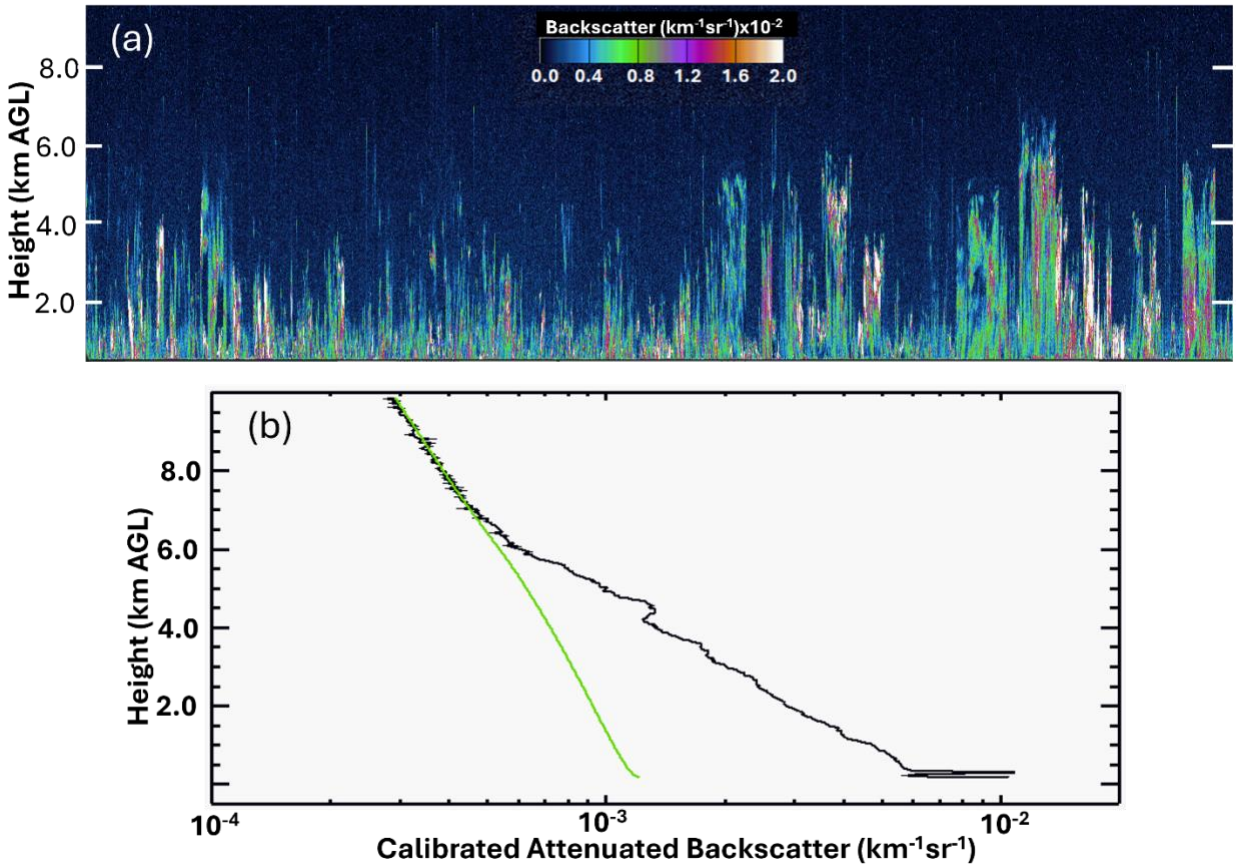

Figure 2. *(a) A sample (50,000) of ICESat-2 calibrated attenuated backscatter profiles from May 2021 that were used to calculate extinction and subsequent ice water content (IWC). (b) The average of the profiles shown in (a) and the corresponding average 532 nm attenuated molecular backscatter profile (green line).*

This image is comprised of 50,000 ICESat-2 profiles from a random selection of profiles that were used for Ice Water Content (IWC) computation from May 2021 and are representative of those that are used for the whole study period. Figure 2b shows the average of the profiles shown in Figure 2a (back line) and the average 532 nm attenuated molecular backscatter (green line). The calibration accuracy of these data is evident by how the average CAB profile above about 6.5 km follows the attenuated molecular profile. Accurate calibration is very important for computing the extinction and IWC.

Though direct measurements of the value of S for diamond dust or CSP over Antarctica are not available, there are surface-based measurements of the physical dimensions and shape of diamond dust obtained at the South Pole (Walden et al. (2003)). Based on these

measurements diamond dust ice crystals are usually comprised of columns, pyramids, and hexagonal plates and are similar enough to cirrus cloud ice crystals such that we can assume the S value is also similar. The value of S for cirrus clouds has been extensively studied since it is very important for determining their optical depth (Whiteman et al., 2000). Based on cirrus clouds in Antarctica, Del Guasta et al. (1993) found that S ranges from 10 to 70 but the median is near 25. There is a slight dependence of S on cloud temperature with higher S values as temperature decreases below -30C.

From the extinction, the IWC can be estimated using the approach from Heymsfield et al. (2014). They found that 532 nm lidar extinction in cirrus clouds is related to IWC (g/m^3) as in Equation 1.

$$IWC = 186.0 * \sigma^{1.15} \quad (1)$$

Where σ is the extinction computed as β*S, where β is the ICESat-2 measured calibrated, attenuated backscatter in units of $m^{-1}sr^{-1}$. If CSP was not detected in a grid box, the extinction is set to zero and thus IWC would also be zero. The IWC calculated at each grid box is then summed over the period being analyzed. From the summed IWC, an estimate of precipitation rate (R_p) can be made by assigning an estimated average fall speed to the ice particles (v).

$$R_p = IWC * v \quad (2)$$

Where R_p has units of $g/m^2/s$. The precipitation rate is obviously very sensitive to the ice particle fall rate. Previous research on columnar ice crystals indicates fall velocities range from 30 cms^{-1} to over 1 m/s depending on the crystal size (Kajikawa, M., 1973). Data presented in Kajikawa (1972) indicate fall velocities for crystals as small as 100 μm to be between 10 and 20 cms^{-1}. Ohtake and Yogi (1979) measured ice crystals at the South Pole during winter. They found that assembled bullet ice crystals were the most common and the largest (about 1 mm or larger) of all crystals observed at the South Pole winter and summer.

Consequently, these crystals are the major contributor to snow accumulation throughout the year. Hexagonal plate crystals and columns smaller than 200 μm were mostly observed under clear skies with a slight wind of 2 to 5 m/s. In summer, such crystals were observed in either stratus fractus clouds or clear skies, but in winter they fell only from clear skies (although the darkness made such observations difficult). However, diamond dust crystals measured at the South Pole are very small with average diameters between 10 and 15 μm (Walden et al., 2003). Fall velocities of diamond dust are likely between 1 and 10 cms^{-1}. Clear -sky precipitation may be a mixture of diamond dust and other larger crystal types. Santachiara et al. (2016) measured ice crystals during clear-sky precipitation events at Dome C and found a mixture of small (10 – 50 μm) and larger crystals (100 μm). Measurements of ice particles averaging around 100 μm in size in an ice fog indicate an average fall speed of 10.7 cms^{-1} (Yagi, 1970) and theoretical calculations of ice particles less than 100 μm in size yield a fall speed of 9.72 cms^{-1} (Mitchell, 1996). Based on the results of the studies cited above, we use an average ice crystal fall speed (*v*) of 0.10 m/s.

From the precipitation rate, precipitation amount (P in mm) is computed for a given time interval by multiplying R_p by the number of seconds in the interval (t) and dividing by the density of water ($\rho = 10^6$ g/m^3). Multiplication by 1000 converts from m to mm.

$$P = R_p * t / \rho * 1000.0 \quad (3)$$

The above computations are performed for every grid box, each of which contains the summed IWC values over the time period t. The resulting Antarctic Plateau-wide precipitation estimates for the period April 1 – October 31, 2021, will be shown in section 3. Before these results are discussed, the next section will present ICESat-2 lidar derived precipitation comparisons with precipitation measurements at Dome C, Antarctica..

2.4 ICESat-2 and Dome C Precipitation Comparison

Table 1. *A comparison of ICESat-2 estimated precipitation (SWE) for the grid box containing Dome C with precipitation measured at Dome C and ERA5 for 8 days in April 2021*.

Day (April 2021)	ICESat-2 Distance from Dome C (km)	ICESat-2 Precipitation (mm)	Dome C Precipitation (mm)	ERA5 Precipitation (mm)
4	19	0.009	0.000	0.000
8	2.7	0.014	0.020	0.029
12	75	0.007	0.103	0.000
16	46	0.015	0.034	0.000
17	73	0.090	0.083	0.004
21	41	0.020	0.054	0.000
25	19	0.006	0.000	0.000
29	3	0.054	0.254	0.000
Total	**-----**	**0.215**	**0.548**	**0.033**

In this section we compare ICESat-2 estimates of clear-sky precipitation near Dome C with precipitation measurements recorded daily at the station (Dreossi et al., 2025). The ICESat-2 precipitation rate is estimated from the lowest 1 km (above the surface) average extinction using Equations 1 and 2 and an average particle fall speed (v) of 10 cms^{-1}. The precipitation amount is computed from Equation 3 using the number of seconds in a day for the time period (t). This is equivalent to the assumption that CSP is falling at a steady rate during the day. As can be seen in Figure 2a, most layers of enhanced backscatter are 2 km or more thick. For a 2 km thick layer, and a falling speed of 0.1m/s, it will take $2x10^4$ seconds for the CSP to come to the surface, which is about five and a half hours. In general, it would take even longer when the horizontal wind is considered. Dome C ceilometer observations for most of the cases also show steady CSP for more than 5 hours. During April 2021 ICESat-2 passed within 100 km of Dome C on 8 separate days as shown in Table 1. While there are no exact coincidences, ICESat-2 passed within 3 km of Dome C on 2 days and within 50 on 4 other days. Also listed in Table 1 are the ICESat-2 estimated, Dome C measured and ERA5 precipitation for those days with the total for the 8 days shown at the bottom. For most days the ERA5 precipitation is zero and the month total is only 0.033 mm. This is considerably less than the ICESat-2 estimate or the Dome C measured amount, but it is not surprising since it is well known that ERA5 does not resolve small scale clear-sky precipitation events (Lavers et al., 2022).

Referring to Table 1, most of the precipitation measured at Dome C occurred on April 12 and 29. The ICESat-2 and Dome C precipitation amounts agree well for most days but not on those two days when Dome C measured considerably more than the ICESat-2 estimated amount. To better understand these discrepancies and verify the ICESat-2 backscatter measurements, Figures 3 and 4 show the ICESat-2 measured CAB and the backscatter measured by the ceilometer at Dome C for April 12 and 29, respectively. On April 12, the ICESat-2 pass occurred at about 12:30 UTC and came within 75 km of Dome C. The ceilometer data shown in Figure 3b indicates that most of the scattering (and assumed ice crystal precipitation) occurred prior to this time. The ICESat-2 precipitation is estimated by the lowest 1 km (above the surface) average CAB and extinction for the portion of Figure 3a within the region indicated by the red vertical lines (a 2-degree latitude x 4-degree longitude box containing Dome C). The average CAB for this area is relatively low which results in a low estimated precipitation and is probably correct for the time and location of ICESat-2 observation but is not representative of the conditions at Dome C, over 75 km away from the ICESat-2 track.

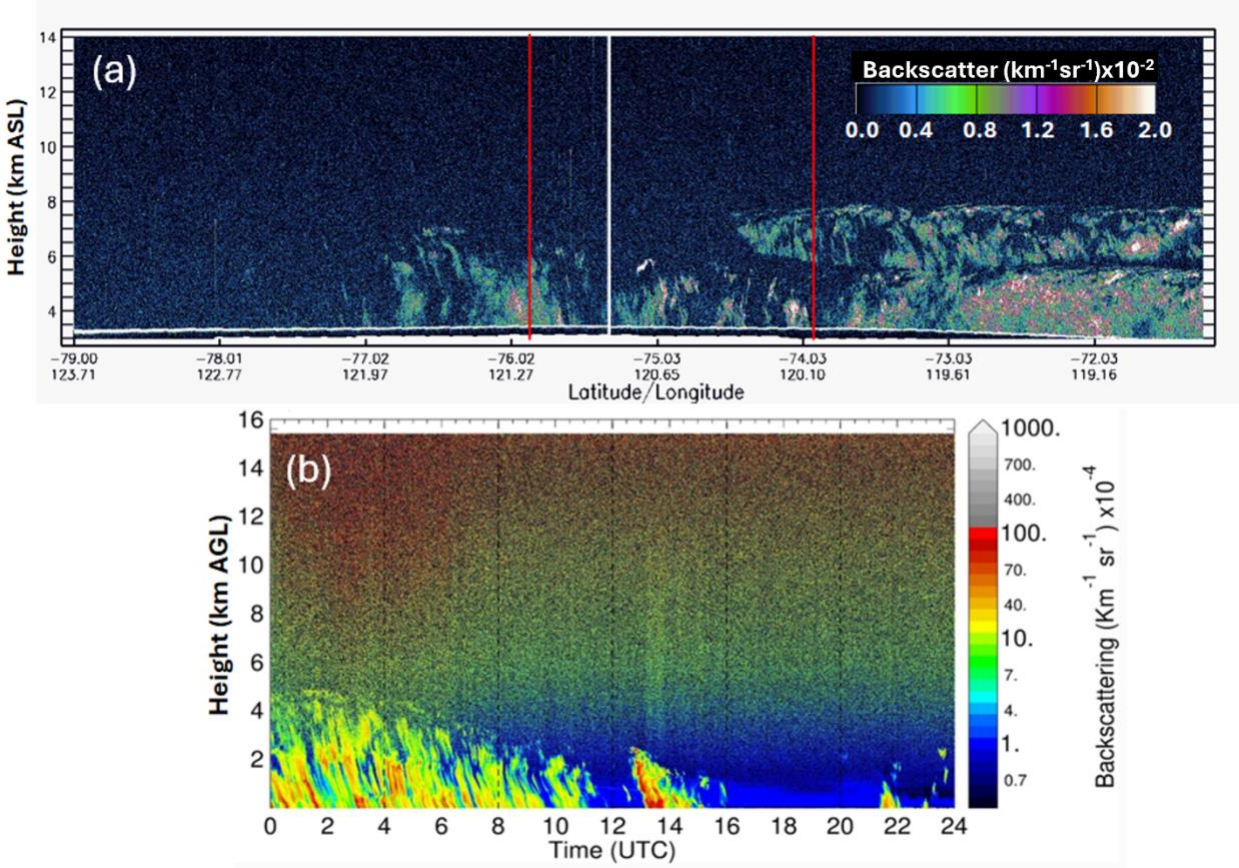

311

312 ***Figure 3****. (a) ICESat-2 measured calibrated, attenuated backscatter (CAB) for the pass closest to*
313 *Dome C on April 12, 2021, 12:29:56 – 12:32:03 UTC. The vertical white line marks the closest*
314 *approach (75 km) to Dome C and the vertical red lines denote the approximate region used to*
315 *compute the 1 km average backscatter as described in the text. (b) The ceilometer backscatter*
316 *measured at Dome C on April 12, 2021. Note the height axis of (a) is km above mean sea level and (b)*
317 *is km above ground level.*

318 The April 12th case illustrates the difficulty in trying to compare ICESat-2 precipitation
319 estimates with a surface point measurement on a particular day. For any given day the
320 ICESat-2 track might be relatively far from the surface station on that day and at a time when
321 precipitation was not occurring. However, the authors feel that these comparisons, though
322 restrictive in their applicability, have value for showing that the enhanced backscatter
323 reaching the surface seen by ICESat-2 is corroborated in the Dome C ceilometer
324 observations.

325

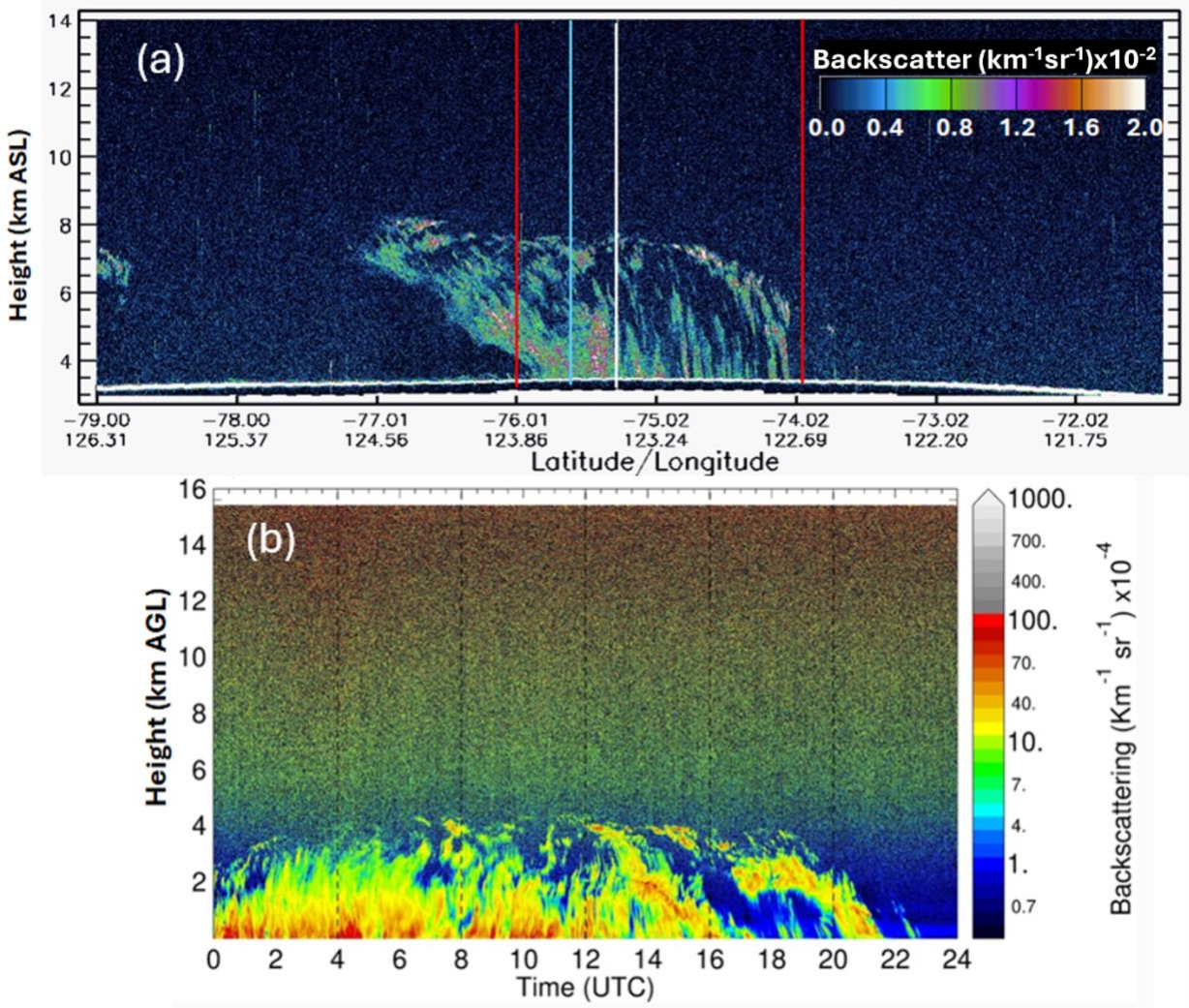

Figure 4*. Same as Figure 3 except for April 29, 2021, 11:30:57 – 11:33:05 UTC and the closest approach to Dome C was 3 km in this case*.

On April 29, the ICESat-2 track came within 3 km of Dome C at about 11:31 UTC. The ICESat-2 measured CAB is shown in Figure 4a together with the Dome C ceilometer data for that day (4b). The latter indicates that elevated scattering consistent with ice crystal precipitation was present virtually all day long and the backscatter structure and magnitude compares well with the ICESat-2 CAB measured at about 11:32 UTC at a distance of just 3 km from Dome C. The ICESat-2 precipitation is estimated from the average CAB and associated extinction in the lowest 1 km above the surface averaged within the region bounded by the two vertical red lines. This average value will be reduced due to the regions of low backscatter seen between the white lines in Figure 4a. As seen in Table 1, the ICESat-2

estimated precipitation is about 4 times less than what was measured at Dome C. In order for the ICESat-2 estimate to match the Dome C observed precipitation amount (0.254 mm), the average 1 km CAB would have to be about $1.6 \times 10^{-5} m^{-1} sr^{-1}$. We reduced the region used to compute the horizontal average to the area between the white line and blue line in Figure 4a. Doing so increased the 1 km average CAB and extinction but only increased the estimated precipitation from 0.054 mm to 0.14 mm, which is still well below what was recorded at Dome C (0.25 mm). The ceilometer data in Figure 4b indicates an average backscatter value in the lowest km above the surface of about $5\text{-}8 \times 10^{-6} m^{-1} sr^{-1}$ prior to 12 UTC. This is very close to the ICESat-2 lowest 1 km average backscatter value between the white and blue lines in Figure 4a ($1 \times 10^{-5} m^{-1} sr^{-1}$) but well below what is needed ($1.6 \times 10^{-5} m^{-1} sr^{-1}$) for the ICESat-2 estimated precipitation to match the observation. This discrepancy could very well be related to the assumed particle fall rate (10 cms^{-1}). If the particle fall rate was in reality twice that value, the ICESat-2 estimated precipitation would be 0.28 mm and very much in agreement with observation.

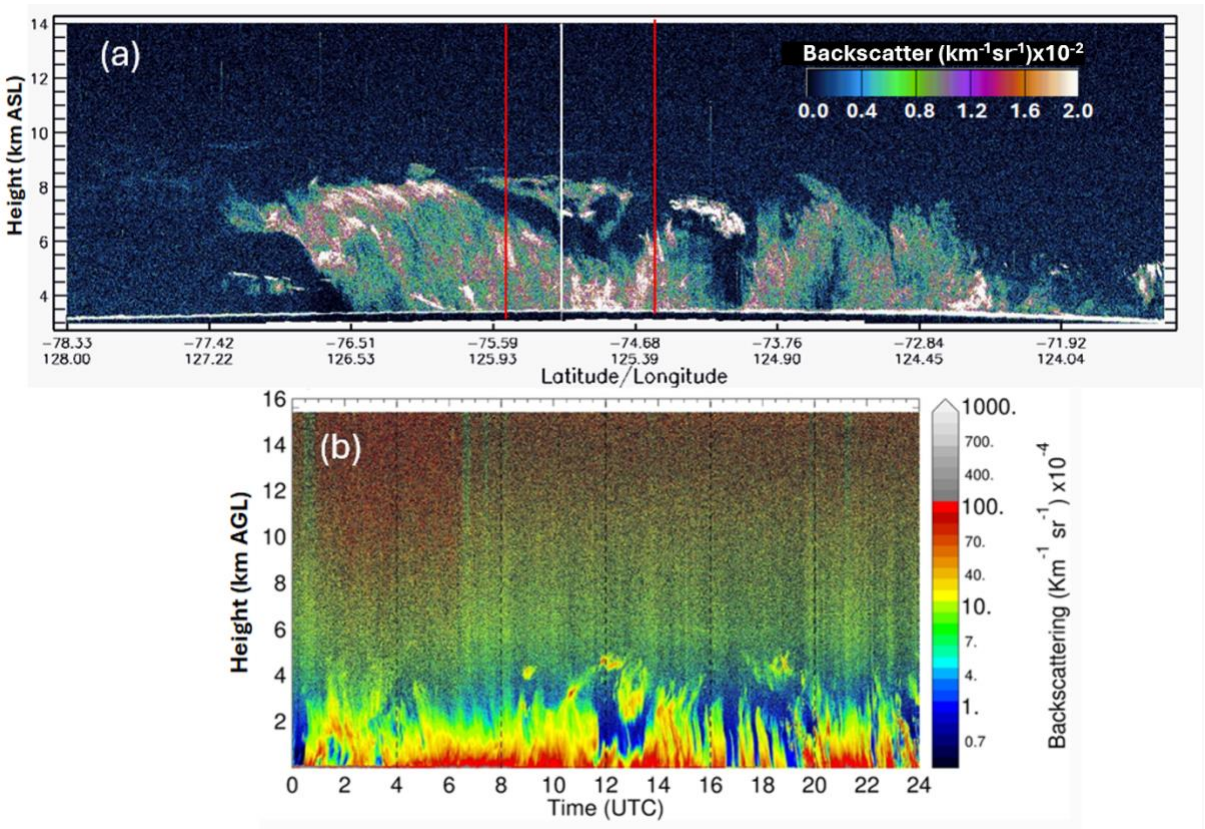

Figure 5*. Same as Figure 3 except for April 17, 2021, 11:56:07 – 11:58:05 UTC and the closest approach to Dome C was 73 km in this case.*

On other days, such as April 17, the ICESat-2 estimated precipitation (0.09 mm) agreed well with the Dome C measured precipitation (0.083 mm). Figure 5a shows the ICESat-2 CAB for a track that came within 73 km of Dome C and the ceilometer data from Dome C on April 17, 2021. The ICESat-2 data show a very large area of enhanced backscatter associated with the precipitation measured at Dome C and is consistent with the elevated backscatter signal seen in the ceilometer data. The relatively large 1 km (above the surface) average CAB data produces the largest ICESat-2 estimated CSP of any day in April. The maximum ICESat-2 backscatter magnitude seen on this day is about 2.0×10^{-5} $m^{-1}sr^{-1}$ and appears more like a cirrus cloud than CSP. The ceilometer data (Figure 5b) indicates that the enhanced backscatter was present the entire day with average CAB values in the lowest 1 km above the surface of between $8.0 \times 10^{-6} m^{-1}sr^{-1}$ and $1.0 \times 10^{-5} m^{-1}sr^{-1}$.

As mentioned in Section 2.2, daily precipitation measurements are made at Dome C. Figure 6 shows the daily precipitation measured at Dome C for April – October 2021 (black line).

This period comprises 214 days, but 70 days are missing (or the reported precipitation was < 0.01 mm) in the Dome C data. In the plot, which shows all 214 days, the precipitation amount of the missing days is set to zero. When precipitation is not reported in the Dome C data, it is because no precipitation was present on the collection platform. This could be that none had fallen or it was blown off by the wind. (G. Dreossi, personal communication). Unfortunately, there is no sure way to distinguish between these two possibilities.

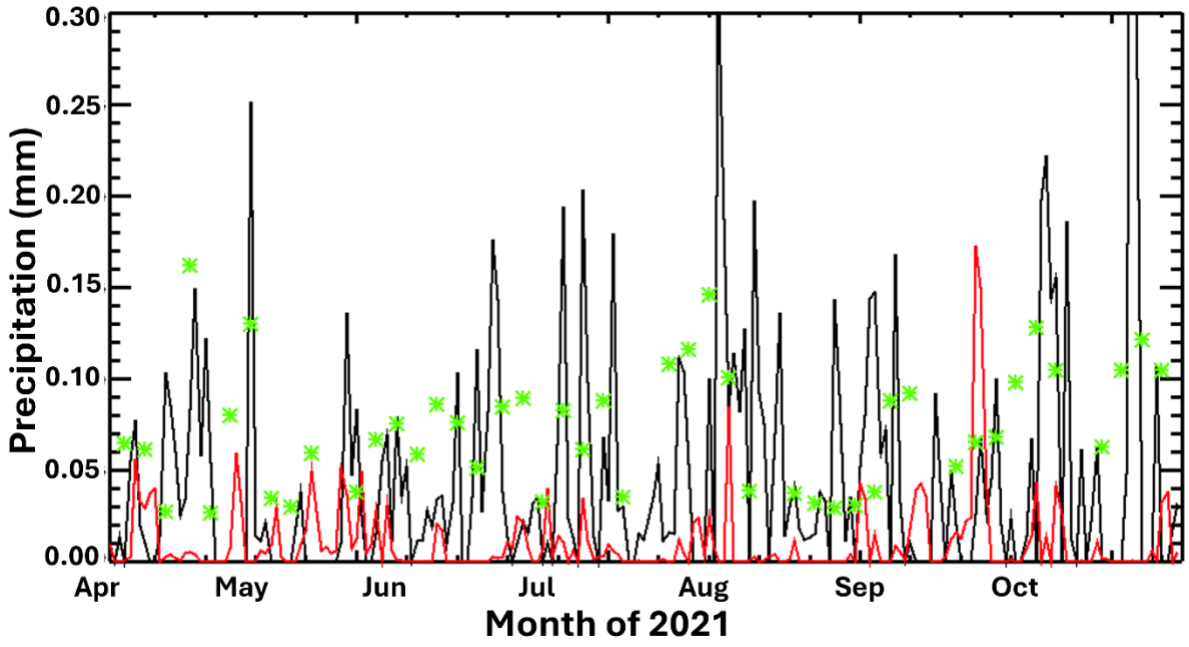

Figure 6. *Daily precipitation measured at Dome C for April 1 – October 31, 2021 (black line), ERA5 daily precipitation at Dome C (red line) and ICESat-2 estimated precipitation amount for the grid box containing Dome C (green asterisks). All amounts are mm SWE.*

Also shown in Figure 6 are the ERA5 daily precipitation amount for the location of Dome C (red line) and the ICESat-2 estimated precipitation for the days that had a pass through the grid box containing Dome C (green stars). Note that ICESat-2 does not pass through the Dome C grid box on every day and some passes could be quite distant from Dome C (as far as ~200 km) . The most striking thing about the measured precipitation at Dome C is the fact that at least some precipitation is reported on most days and that usually the amounts are very small (< 0.15 mm). On only 13 days was the measured precipitation greater than 0.15 mm (SWE). The total amount of precipitation measured at Dome C over this period was 9.9

mm recorded on 144 of the 214 days. If we assume the other 70 days in the period had no precipitation, then the precipitation frequency at Dome C is 144/214 or 67%. This is close to the ICESat-2 CSP frequency for the Dome C grid box of 71%. For the entire year of 2021 only 14.6 mm of precipitation was measured at Dome C. Note that the ERA5 precipitation is almost always less than 0.05 mm SWE and the total for the April – October period was only 2.2 mm, well below both Dome C observation (9.9 mm) and the ICESat-2 CSP estimate (8.5 mm).

3. ICEsat-2 East Antarctic Plateau CSP

In this section, the technique to compute CSP using ICESat-2 data discussed in Section 2.2 is used to generate a CSP amount for the period April 1 – October 31, 2021, over the East Antarctic Plateau. We define the Plateau as the region of East Antarctica that exceeds 2500m in height (AMSL). This area is known to be the region where CSP is most frequent and where CSP accounts for a sizeable portion of the annual precipitation. The time period considered is limited to months of the year where solar background noise is either absent or at a relatively low level. The ICESat-2 backscatter signal received from diamond dust and CSP is generally so low that it will be completely lost in the presence of appreciable solar background noise. This is a limitation of ICESat-2 specifically. Other satellite lidars such as CALIPSO (Cloud-Aerosol Lidar Infrared Path-finder Satellite Observations) or EarthCARE (Earth Cloud Aerosol and Radiation Explorer) may not be as limited, but the analysis of those data is beyond the scope of this paper.

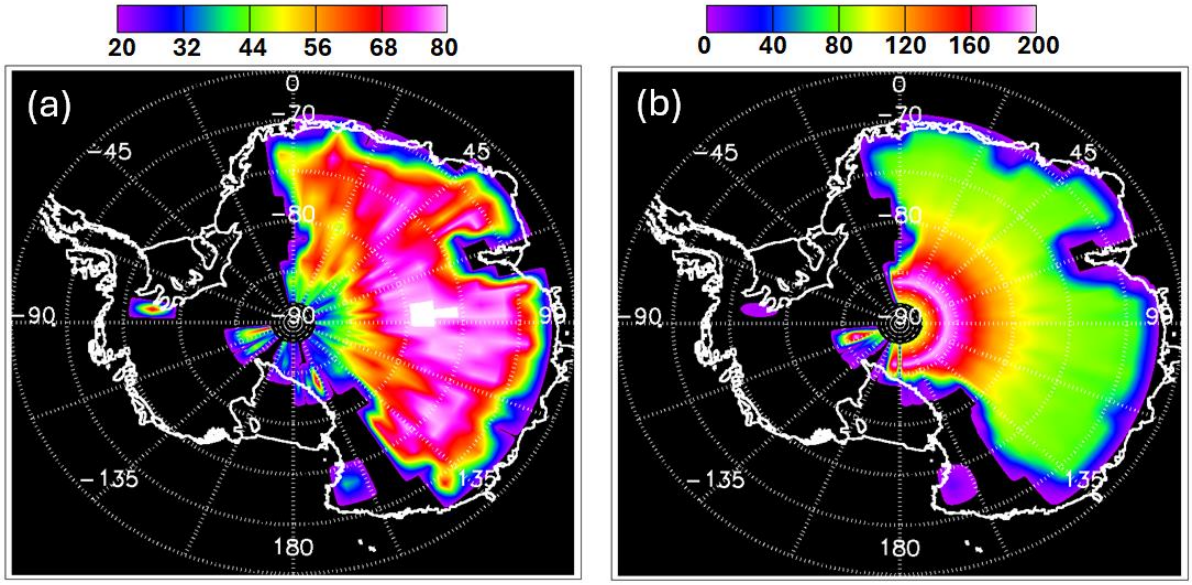

Figure 7*. (a) The percentage of observations that contained ICESat-2 detected clear-sky precipitation and (b) the number of observations per grid box.*

Figure 7a shows the frequency of detected CSP. This is computed by noting for each grid box whether CSP was detected or not. CSP is considered detected when the lowest 1 km above the surface average CAB for the entire grid box exceeds the threshold (2 times the molecular scattering value). If CSP is detected, the CSP grid box count is incremented as is the observation grid box count. If CSP is not detected in a grid box, only the observation count is incremented. After all the granules for the time period under consideration are analyzed, the CSP frequency is computed by dividing the CSP grid count by the observation grid count. Figure 7a shows that there is not a large range of CSP frequency as most of the Plateau has a relatively high frequency of about 70%. The maximum frequency of about 80% occurs very near to Dome A (80.37S, 77.35E) which is the highest point in East Antarctica (4087 m). The number of observations per gid box is shown in Figure 7b. The observation count is kept for each grid box and is incremented when at least 100 backscatter profiles occur in the box from a given ICESat-2 overpass. The 92-degree inclination polar orbit of ICESat-2 provides coverage to 88S where the maximum number of observations occur (over 200 per grid box). The number of observations decreases northward, but for most of the Plateau, the observation count is greater than 100 per grid box.

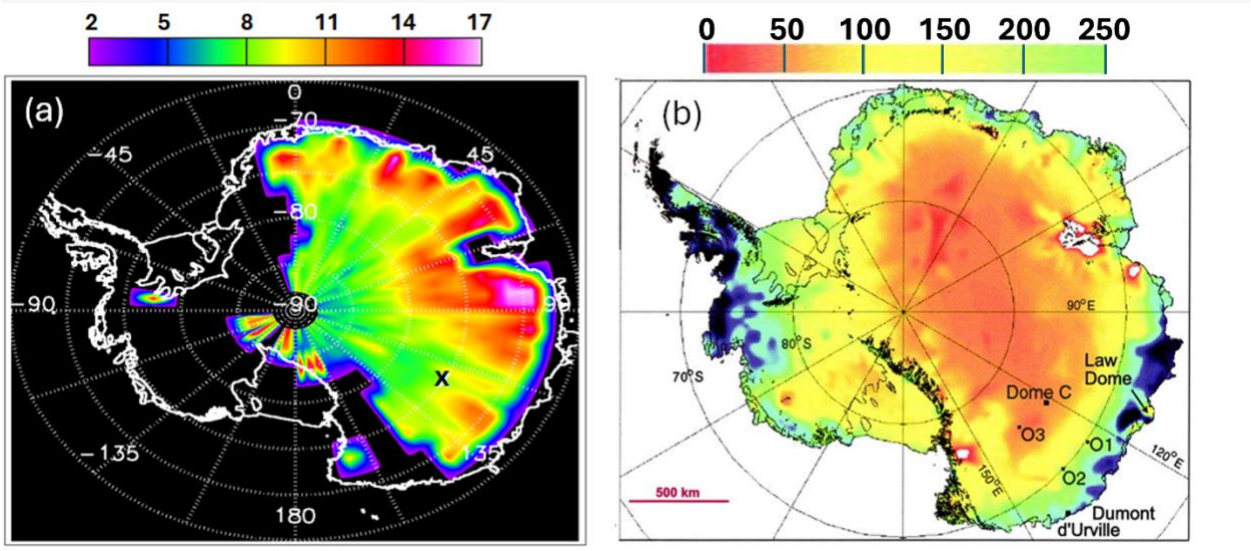

Figure 8. *(a) ICESat-2 estimated clear-sky precipitation (mm SWE) over the East Antarctica plateau for the period April 1 to October 31, 2021. The location of Dome C (75.1S, 123.3E) is indicated by the black 'X' drawn on the image. (b) Antarctic annual precipitation minus evaporation (mm SWE) from Massom et al., 2003.*

Applying the method discussed in Section 2.2 to the ICESat-2 data for the April – October 2021 period results in the Plateau-wide estimated CSP shown in Figure 8a. The precipitation total amount ranges from about 5-8 mm south of about 80S and increases toward the north with maximum values of 18-20 mm near 70S, 90E. The increase in CSP toward the coasts and lower elevation is consistent with the likely larger availability of moisture compared to the higher regions of the Plateau. Also, ice particle extinction in cirrus clouds shows a notable increase as temperature increases (Heymsfield et al., 2014). The grid box containing Dome C, the location of which is noted by the black 'X' (75.1S, 123.3E) in Figure 8a, has a total ICESat-2 estimated CSP amount of 8.5 mm SWE for April – October. Figure 8b shows the annual precipitation for Antarctica based on measurements and models (Massom et al., 2003). The precipitation amount of the reddish-orange area is below 100 mm/year and there are regions in the highest portions of the Plateau where precipitation is less than 50 mm/year. The reddish-orange area includesthe region covered by the ICESat-2 precipitation grid shown in Figure 8a. While the April – October ICESat-2 estimated precipitation is very small, it must be realized that large parts of the East Antarctic interior receive on average less than 50 mm SWE of precipitation for the entire year (Palerme et al, 2014). In fact, some areas

receive less than 20 mm per year (Krinner et al., 2007; Palerme et al., 2017). Thus, the ICESat-2 estimated CSP accounts for a significant portion of the total annual precipitation thought to fall in that region.

4. Uncertainty Analysis

The ICESat-2 estimates of CSP depend on several factors that are not well known. The two most important are the falling speed and the extinction to backscatter ratio (S) of the ice particles that comprise CSP. The ICESat-2 estimated precipitation is directly related to the particle fall speed (through Equation 2). The particle fall speed used here – 10 cms^{-1} – could vary considerably as a function of atmospheric conditions and particle physical characteristics (i.e. size and shape). The extinction is computed from the measured ICESat-2 calibrated, attenuated backscatter using an extinction to backscatter ratio (S) of 30 sr. This value also varies with atmospheric conditions (mainly temperature) and ice particle properties. Also important is the accuracy of estimating the ice water content (IWC) of the CSP from the lidar measured extinction. Given these unknowns it is difficult to assign uncertainty to the ICESat-2 estimated CSP. Table 2 lists our best estimate of the uncertainty of the various components of the ICESat-2 precipitation calculation.

Table 2. *Estimated uncertainty of components of the ICESat-2 precipitation calculation.*

Component	Estimated Uncertainty (%)
Calibrated Backscatter (β)	5
Extinction to Backscatter Ratio (S)	20
IWC from Extinction (Eqn 1)	20
Ice Particle Fall Speed (v)	80

The overall ICESat-2 precipitation amount uncertainty is then the square root of the sum of the squares of the individual components, which equates to 85%. This value is obviously

dominated by the particle fall speed but uncertainty in the extinction to backscatter value and accuracy of estimating IWC from lidar extinction are also important.

While the precipitation amount uncertainty is obviously very high, these results are the first of their kind and represent the only Antarctic Plateau-wide estimates of clear-sky precipitation available. Reduced uncertainty in the ICESat-2 CSP estimates can be achieved by in-situ measurements of particle fall speeds and extinction to backscatter values of clear-sky precipitation. The spatial distribution and frequency of ICESat-2 estimated CSP has much higher confidence and are an important contribution to the understanding of Antarctic CSP in and of themselves.

5. Discussion

Results of prior studies have indicated that clear-sky precipitation (CSP) is very frequent in the Interior of East Antarctica. Numerous authors have estimated that CSP frequency is near or exceeds 80% (Radok and Lile,1977; Dittmann et al., 2016; Walden et al., 2003). The results presented here are consistent with these numbers. We find that over much of the East Antarctic Plateau, the frequency of CSP is greater than 70% with the highest regions reaching a frequency of 80% and appears to be related to elevation (higher elevation, higher frequency). During the April – October 2021 period, Dome C did not experience a precipitation event exceeding 0.5 mm and the total precipitation was just 9.9 mm SWE. The ICESat-2 estimate for the grid box containing Dome C was 8.5 mm SWE. However, it is noted that the precipitation measured at Dome C could include blowing snow particles and hoar frost. We attempted to remove the hoar frost contribution by only considering precipitation amounts greater than 0.01 mm. Blowing snow frequency is relatively low at Dome C compared to other locations in Antarctica (Palm et al., 2011; 2018; Ganeshan et al., 2022). Using the blowing snow parameter (*bsnow_h*) on the ICESat-2 ATL09 data product, the average blowing snow frequency in the grid box containing Dome C was 20% for the period April 1 – October 31, 2021. Thus, contributions to the precipitation amount from blowing snow are likely not zero, but unfortunately the magnitude cannot be determined. Similarly, wind blowing snow/ice particles off the platform (on which precipitation is collected) could

also affect the amount of precipitation measured. The collection platform is surrounded by an 8 cm rail which hopefully mitigates this effect but would not eliminate it. In addition, the average wind speed for the study period measured by the automated weather station (AWS) at Dome C was 3.2 ms^{-1}, indicating wind at Dome C is generally not a concern. Notwithstanding these problems, it is clear that precipitation at Dome C is extremely light and, in at least winter months, is likely dominated by frequent, very light events that are indicative of CSP.

6. Summary and Conclusion

The objective of this study is to show that the frequency and magnitude of clear-sky precipitation can be estimated by satellite lidar. The presence of clear-sky precipitation or CSP is defined as enhanced backscatter in contact with the surface. Enhanced backscatter is defined as the average backscatter in the lowest 1 km above the surface that exceeds 2 times the molecular scattering value. This definition of CSP would include optically thin cirrus-like ice clouds in contact with the surface and differs from the normal definition which describes it as ice crystals falling from an otherwise clear sky. Using this 1 km average backscatter and an assumed extinction to backscatter ratio of ice particles (30 sr) the average extinction can be computed. From the extinction the ice water content (IWC, g/m^3) can be estimated from an equation developed by Heymsfield et al. (2014). The precipitation rate ($g/m^2/s$) is obtained by multiplying the IWC by the fall speed (ms^{-1}) of the ice particles. Precipitation amount is then obtained by multiplying the precipitation rate by the length of the time period being analyzed in seconds and dividing by the density of water.

The results show that most of the East Antarctic Plateau has a relatively high frequency of CSP averaging about 70%. The maximum frequency of CSP (80%) occurs very near to Dome A (80.37S, 77.35E) which is the highest point in East Antarctica (4087 m). The precipitation frequency at Dome C, measured by the number of days that had measurable precipitation between April 1 and October 31, 2021, was 67.3%. This agrees well with the ICESat-2 CSP frequency for that location (71%). The estimated CSP amount does not show the same spatial distribution as the CSP frequency. but rather has a distinct south to north gradient. It

ranges from about 5-8 mm south of about 80S and increases toward the north with maximum values of 18-20 mm near 70S, 90E. This increase in CSP nearer the coast may be due to warmer and moister air compared to that over the higher portions of the Plateau. Though the ICESat-2 estimated precipitation is small, it is a significant fraction of the total annual precipitation thought to fall in this region.

Comparisons with Dome C precipitation measurements for 8 days in April 2021 were made. General agreement was seen except for 2 days when the Dome C precipitation was considerably greater than the ICESat-2 estimation (April 12th and 29th). However, on the 12th the ceilometer data at Dome C indicated most of the precipitation had occurred prior to the time of the ICESat-2 observation which also only came within 75 km of Dome C. On the 29th of April Dome C precipitation was about 5 times the ICESat-2 estimated CSP. The cause of this discrepancy is not clear but underscores the difficulty in using one satellite overpass to estimate and compare precipitation amount with a single ground measurement. The total precipitation measured at Dome C for the April – October period was 9.9 mm SWE. The ICESat-2 estimated CSP amount for the grid box containing Dome C was 8.5 mm SWE. Given the uncertainty in both the ICESat-2 estimate and the Dome C measurement, this can be considered as good agreement. It should be noted that the main uncertainty in these calculations is related to the fall speed of the ice crystals comprising CSP. A doubling of the value used here (10 cms) will result in a doubling of the clear-sky precipitation amounts. Thus, obtaining accurate fall speeds of CSP ice particles at locations representative of the Antarctic plateau like Concodia Station, Dome Fuji (77°19'S 39°42'E) and the South Pole is very important to reducing the large uncertainty in the clear-sky precipitation amounts presented here.

In conclusion, this study presents a method to estimate the frequency and magnitude of clear-sky precipitation over the East Antarctic Plateau using ICESat-2 calibrated backscatter measurements. To our knowledge this work is the first attempt to use satellite lidar remote sensing to estimate the frequency and magnitude of clear-sky precipitation over a large region of Antarctica. It is acknowledged that the results have a relatively large degree of uncertainty, but we feel they are nonetheless valuable because models are unable to reliably

predict CSP amount and satellite lidar measurements of CSP may be useful in constraining and improving model performance. In addition, these measurements can be helpful for ice sheet mass balance studies and possibly for the interpretation of ice core samples for paleoclimatology research.

Acknowledgements

This work was funded by NASA Contract Number 80NSSC20K0969. The authors thank Dr. Thorsten Markus for providing the funding and moral support that enabled the completion of this work. The authors would also like to thank Giuliano Dreossi, Barbara Stenni, Virginia Ciardini and Paolo Grigioni for their help with obtaining and interpreting the Dome C data. The Dome C **Dataset and information are achieved by the Italian Antarctic Meteo-Climatological Observatory (IAMCO) https://www.climantartide.it of the PNRA**

Open Research

The ICESat-2 ATL09 data are publicly available at the National Snow and Ice Data Center at https://nsidc.org/data/atl09/versions/6. The Dome C ceilometer data can be found here: https://www.climantartide.it/dataonline/ceilometer. The Dome C precipitation data are available at https://doi.pangaea.de/10.1594/PANGAEA.972031?format=textfile and the AWS data can be found here: https://www.climantartide.it/dataonline/aws/. The ERA5 data were obtained from the climate data store at ERA5 hourly data on single levels from 1940 to present. The software used to process the ICESat-2 data can be obtained by contacting the corresponding author at stephen.p.palm@nasa.gov

References

Abdalati, W., Zwally, H. J., Bindschadler, R., Csatho, B., Farrell, S. L., Fricker, H. A., et al. (2010). The ICESat-2 altimetry mission. *IEEE Transactions on Geoscience and Remote Sensing*, *98*(5), 735–751. https://doi.org/10.1109/JPROC.2009.2034765

Bromwich D. (1988): Snowfall in high southern latitudes. *Rev Geophys* 26:149–168

Del Guasta, M., M. Morandi and L. Stefanutti, (1993): One Year of Cloud Lidar Data From Dumont d'Urville (Antarctica) 1. General Overview of Geometrical and Optical Properties, *J. Geophys. Res.*, 98, 18,575 – 18,587

Dittmann, A., E. Schlosser, V. Masson-Delmotte, J. G. Powers, K. W. Manning, M. Werner, and K. Fujita (2016): Precipitation regime and stable isotopes at Dome Fuji, East Antarctica, *Atmos. Chem. Phys.*, 16, 6883–6900, 2016 www.atmos-chem phys.net/16/6883/2016/ doi:10.5194/acp-16-6883-2016

Dreossi, G, M. Masiol, B. Stenni, D. Zannoni, C. Scarchilli, et al. (2024) A decade (2008-2017) of water stable-isotope composition of precipitation at Concordia Station, East Antarctica, *The Cryosphere*, 18, 3911–3931, https://doi.org/10.5194/tc-18-3911-2024

Dreossi, Giuliano; Stenni, Barbara; Masiol, Mauro; Zannoni, Daniele; Ollivier, Inès (2025): Water stable isotopic composition of precipitation at Concordia Station (Dome C), East Antarctica (2017-2021) [dataset]. PANGAEA, https://doi.org/10.1594/PANGAEA.972031

Ekaykin, A. A., Lipenkov, V. Y., Kuzmina, I. N., Petit, J. R., Masson-Delmotte, V., and Johnsen, S. J.: The changes in isotope composition and accumulation of snow at Vostok station, East Antarctica, over the past 200 years, *Ann. Glaciol.*, 39, 569–575

Ganeshan, M., Y. Yang, S. P. Palm, 2022: Impact of Clouds and Blowing Snow on Surface and Atmospheric Boundary Layer Properties over Dome C, Antarctica. *J. Geophys. Res.*, 127, e2022JD036801. https://doi.org/10.1029/2022JD036801.

Grenier, P., J.P. Blanchet, and R. Mun˜oz-Alpizar (2009): Study of polar thin ice clouds and aerosols seen by CloudSat and CALIPSO during midwinter 2007, *J. Geophys. Res.*, 114, D09201, doi:10.1029/2008JD010927

Grigioni, P., Ciardini, V., Camporeale, G., De Silvestri, L., Iaccarino, A., Proposito, M., & Scarchilli, C. (2022). Dati del Celiometro CL51 presso la Base CONCORDIA STATION (DomeC). ENEA. https://doi.org/10.12910/DATASET2022-006

607 Heymsfield, A. D. Winker, M. Avery, M. Vaughan, G. Diskin, M. Deng and V.Mitev, (2014):
608 Relationships between Ice Water Content and Volume Extinction Coefficient from In Situ
609 Observations for Temperatures from 0 to -86 °C: Implications for Spaceborne Lidar
610 Retrievals, *J. Appl. Meteor. Climatol.*, 53, 479-505, DOI: 10.1175/JAMC-D-13-087.1

611 Hogan, A. W. (1976): Summer ice crystal precipitation at the South Pole. *J. Appl. Meteor.,*
612 **14,** 246–249.

613 Intrieri, J. M. and M. Shupe (2004): Characteristics and Radiative Effects of Diamond Dust
614 over the Western Arctic Ocean Region, *J. Clim*, 17, 2953-2960.

615 Kajikawa, M., 1973:Laboratory measurement of falling velocity of individual ice crystals . *J.*
616 *Meteor. Soc. Japan*, 51, 263-272 .
617 ----------1976: Observation of falling motion of columnar snow crystals. *J. Meteor* .
618 *Soc. Japan*,54, 276-284.
619
620 Khvorostyanov, V.I, and J. A. Curry, (2002). Terminal velocities of droplets and crystals:
621 power laws with continuous parameters over the size spectrum. *J. Atmos. Sci.*, 59

622 Krinner, G., O. Magand,, I. Simmonds, C. Genthon and J. -L. Dufresne: Simulated Antarctic
623 precipitation and surface mass balance at the end of the twentieth and twenty-first
624 centuries (2007*) Clim. Dyn.* 28:215–230 DOI 10.1007/s00382-006-0177-x

625 Lavers, D.A., Simmons, A., Vamborg, F. and Rodwell, M.J., 2022. An evaluation of ERA5
626 precipitation for climate monitoring. Quarterly Journal of the Royal Meteorological Society,
627 148(748), pp.3152-3165.

628 Markus, T., Neumann, T., Martino, A., Abdalati, W., Brunt, K., Csatho, B., et al. (2017). The
629 ice, cloud, and land elevation satellite-2 (ICESat-2): Science requirements, concept, and
630 implementation. *Remote Sensing of Environment*, *190*, 260–273.
631 https://doi.org/10.1016/j.rse.2016.12.029

Massom, R. A., M. J. Pook, J. C. Comiso, N. Adams, J. Turner, T. Lachlan and T. T. Gibson (2003) Precipitation over the Interior East Antarctic Ice Sheet Related to Midlatitude Blocking-High Activity. *J. Clim*., 17, 1914-1928

Ohtake, T. and Yogi, T., 1979. Winter ice crystals at the South Pole. *Antarct. J. U. S*. 14, 201–203.

Mitchell, D. L., 1996: Use of Mass- and Area-Dimensional Power Laws for Determining Precipitation Particle Terminal Velocities. *J. Atmos. Sci.*, **53**, 1710–1723, https://doi.org/10.1175/1520-0469(1996)053<1710:UOMAAD>2.0.CO;2.

Palerme, C., J. E. Kay, C. Genthon, T. L'Ecuyer4 N. B. Wood, and C. Claud (2014) How much snow falls on the Antarctic ice sheet? *The Cryosphere*, 8, 1577–1587, 2014 www.the-cryosphere.net/8/1577/2014/ doi:10.5194/tc-8-1577-2014

Palerme, C. Genthon, C. Claud, J. E. Kay, N. B. Wood and T. L'Ecuyer (2017) Evaluation of current and projected Antarctic precipitation in CMIP5 models, Clim Dyn (2017) 48:225–239, DOI 10.1007/s00382-016-3071-1

Palm, S. P., Yang, Y., Spinhirne, J. D., & Marshak, A. (2011). Satellite remote sensing of blowing snow properties over Antarctica. *J. Geophys. Res. Atmos.*, *116*(D16), D16123. https://doi.org/10.1029/2011JD015828

Palm, S.P., V. Kayetha and Y. Yang (2018) Toward a Satellite-Derived Climatology of Blowing Snow Over Antarctica. *J. Geophys. Res. Atmos*.**123,18**, 10,301-10,31

Palm, S. P., Yang, Y., Herzfeld, U., Hancock, D., Hayes, A., Selmer, P., et al. (2021). ICESat-2 atmospheric channel description, data processing and first results. *Earth and Space Science*, *8*, e2020EA001470. https://doi.org/10.1029/2020EA001470

Radok, U. and R. C. Lile (1977): A Year of Snow Accumulation at Plateau Station, *Antarctic Research Series, Meteorological Studies at Plateau Station, Antarctica*, 25, 17-26.

Santachiara, G, F. Belosi, F. Prodi (2016): Ice crystal precipitation at Dome C site (East Antarctica) *Atmospheric Research*, 167 108–117

Smiley, V.N., B.M. Whitcomb, B.M. Morley and J.A. Warburton (1980): Lidar Determinations of Atmospheric Ice Crystal Layers at the South Pole during Clear-Sky Precipitation J. Appl. Meteor., 19, 1074-1090.

Stenni, B., C. Scarchilli, V. Masson-Delmotte, E. Schlosser, V. Ciardini, G. Dreossi, P. Grigioni, M. Bonazza, A. Cagnati, D. Karlicek, C. Risi, R. Udisti, and M. Valt (2016): Three-year monitoring of stable isotopes of precipitation at Concordia Station, East Antarctica, *The Cryosphere*, 10, 2415–2428, www.the-cryosphere.net/10/2415/2016/ doi:10.5194/tc-10-2415-2016

Walden, V.P., S.G. Warren and E. Tuttle, (2003) Atmospheric Ice Crystals over the Antarctic Plateau in Winter. *J Appl. Meteor.*, 42, 1391-1405

Whiteman, D. N., B. Demoz and Z. Wang, (2004) Subtropical cirrus cloud extinction to backscatter ratios measured by Raman Lidar during CAMEX-3, Geophys. Res. Lett., 31, L12105, doi10.1029/2004GL020003

Yagi, T., (1970) Measurement of the Fall Velocity of Ice Crystals Drifting in Supercooled Fog, J. Meteor. Soc. Japan, 48, 287-292